COMPUTATIONAL ASSESSMENT OF ATMOSPHERIC CARBON DIOXIDE DISPERSION FROM IBOM POWER THERMAL PLANT USING GAUSSIAN PLUME MODELLING TECHNIQUES

[1]JIMOH, O. R., [2]OGBADA, N., & [3]SALIHU, N. O.
[1,3]Department of Mathematics, School of Physical Sciences,
Federal University of Technology Minna, Nigeria.
[2]Department of Mathematics and Statistics, School of Pure and Applied Sciences,
Federal University of Technology Ikot Abasi, Nigeria.
E-mails: razaq.jimoh@futminna.edu.ng, nathanielogbada@gmail.com,
so.nasiru@futminna.edu.ng
Phone Nos: +234 807 780 8699, +234 803 578 9694 +234 810 628 7010

Abstract
Atmospheric carbon dioxide (CO_2) emissions from gas-fired thermal power plants contribute to air quality degradation and long-term climate change. In Nigeria, the increasing reliance on natural gas for electricity generation necessitates the assessment of CO_2 dispersion patterns around power plant facilities. This research paper contributes to sustainable development in Nigeria by presenting a quantitative assessment of atmospheric CO_2 dispersion from the Ibom Power Thermal Plant, using Gaussian plume modelling techniques. The governing advection–diffusion equation was solved analytically using collocation technique and implemented in MAPLE for simulation and visualization. A sensitivity analysis was conducted on model parameters such as emission rate, wind velocity, reaction rate, stack height and atmospheric stability classes. The results identify a critical impact zone between 2000–5000m downwind where ground-level CO_2 is likely to be highest, especially under stable atmospheric conditions. Increased wind speed and stack height significantly reduce concentrations, while higher emission rates and stable atmospheric conditions increase CO_2 concentration. The reaction term introduces additional reduction in CO_2 concentration with distance, although its effect is smaller compared to meteorological and source parameters. The findings support the placement of sensitive receptors such as residential areas, schools, and hospitals outside the high-impact region and demonstrate the usefulness of Gaussian-based dispersion modelling for environmental impact assessment.

Keywords: Gaussian plume model, atmospheric dispersion, pollutant modelling, carbon dioxide emission, collocation method.

Introduction

The rising concentration of atmospheric carbon dioxide (CO_2) has become a major environmental concern considering its contribution to global warming and climate change (Nunes, 2023). According to the International Energy Agency (IEA), CO_2 is the most prevalent pollutant among the various greenhouse gases emitted, and its contribution to global warming and climate change is well documented (IEA, 2023). The continued emission of CO_2 from fossil fuel–based energy systems therefore presents significant environmental and public health challenges worldwide.

Natural gas-fired power plants emit significantly less CO_2 than coal-fired plants per unit of electricity generated. On the average, natural gas emits about 50–60% less CO_2 than coal (USEPA, 2025). Despite this relative advantage, natural gas remains a substantial source of CO_2 emissions, especially when lifecycle emissions, including methane leakage during extraction and transport are considered (Alvarez *et al.,* 2018). As a result, the dispersion of CO_2 from thermal power plants remains an important subject for environmental assessment and mitigation planning.

In Nigeria, the power generation sector accounts for a significant portion of CO_2 emissions. Emodi and Boo (2017) observed that the growing reliance on gas-fired power plants, while cleaner than alternatives, continues to elevate Nigeria's carbon footprint. Nigeria is a regional leader in fossil fuel power generation and its power sector emissions are projected to grow in the absence of large-scale transitions to renewable energy (Awodumi & Adewuyi, 2020). Natural gas is the dominant fuel for grid electricity in the country, and this reliance is expected to persist in the near future. Having a clear understanding of the dispersion behaviour of CO_2 from gas-fired power plants in Nigeria is important for environmental impact assessment, regulatory decision-making, and sustainable urban development.

The Ibom Power Plant, a 191 megawatts (MW) gas-fired facility situated in Ikot Abasi, Akwa Ibom State, Nigeria, is one of many facilities where fast energy demand is matched by rising environmental concerns. On October 27, 2015, Ibom Power was given approval by the Nigerian Electric Regulatory Commission (NERC) to add 500 megawatts to its current generating power, with installation to begin in 2025 (The Guardian, 2015). This additional generating power will increase the emission rate of pollutants, thereby, increasing the overall pollution profile of the region. This anticipated expansion makes it necessary to evaluate how increased emissions may affect the spatial distribution of CO_2 concentrations around the facility, particularly with respect to residential and environmentally sensitive areas.

Over the years, various atmospheric dispersion models have been developed to predict the behaviour of pollutants in the air. Traditional models such as the Gaussian Plume Model (Al-Naser and Khalaf, 2025) and Computational Fluid Dynamics (CFD) models (Pantusheva *et al.,* 2022) have been widely used in air quality assessments. The Navier-Stokes equations (Lacome *et al.,* 2023) are also fundamental in describing fluid motion in atmospheric dispersion studies. Among these models, the Gaussian plume model remains one of the most established tools for modelling pollutant dispersion in the atmospheric boundary layer under steady-state conditions. This is due to its computational simplicity and practical reliability (Seinfeld & Pandis, 2016). The model has been widely applied in different contexts, including studies by Happiness *et al.* (2019) on the Omotosho power plant and Abiye *et al.* (2016) on industrial emissions in Ile-Ife, where Gaussian-based approaches were successfully used to estimate pollutant dispersion patterns. The use of Pasquill–Gifford stability classes (Turner, 1994) to parameterize horizontal and vertical dispersion remains standard practice.

Despite the widespread application of Gaussian plume models, their use in assessing CO_2 dispersion from Nigerian gas-fired thermal power plants remains limited. This study addresses this gap by developing a localized model that integrates site-specific emission and meteorological data to predict spatial CO_2 concentration fields under steady-state conditions. By applying the Gaussian plume model and validating its analytical formulation through a collocation-based numerical framework, this work provides a localized, quantitative assessment of CO_2 dispersion for a major Nigerian thermal power facility and offers insights relevant for environmental management and land-use planning.

Model Description

Although the analytical solution of the advection–diffusion equation leads to the Gaussian plume formulation, it is instructive to examine whether this closed form solution can be reproduced through a numerical framework. The advection–diffusion equation represents conservation of mass for a passive scalar subject to transport by a mean flow (advection) and spreading by turbulent fluctuations (diffusion). Under steady-state conditions with constant wind speed and homogeneous turbulence, its fundamental solution for a continuous point source takes a Gaussian form in the transverse and vertical directions.

For this reason, the collocation method, which belongs to the class of weighted residual techniques for solving differential equations, was used. In the collocation approach, the solution is approximated by a trial function containing unknown parameters, and the governing equation is enforced exactly for selected test functions or moments. This procedure reduces the partial differential equation to a system of ordinary differential equations for the plume parameters, which can be solved analytically or numerically. The collocation method thus provides a constructive approximation framework that reproduces the Gaussian plume solution and offers a pathway for extension to more general transport problems where closed-form solutions are unavailable.

The conceptual link between the general advection–diffusion equation and the Gaussian plume formulation has been established in existing literatures, demonstrating that under steady conditions, advective transport with turbulent diffusion leads to Gaussian concentration profiles (Lupini & Tirabassi, 1967).
Given the advection–diffusion equation:

$$\frac{\partial(C)}{\partial t} + U\frac{\partial C}{\partial x} = D_x\frac{\partial^2 C}{\partial x^2} + D_y\frac{\partial^2 C}{\partial y^2} + D_z\frac{\partial^2 C}{\partial z^2} + S(x,y,z) - k_r C \quad (1)$$

Where C is the concentration of CO_2 at location (x,y,z), U is the mean speed in x–directions, D_x, D_y, D_z are the diffusion coefficients in the x, y and z directions, $S(x,y,z)$ is the source term for CO_2 emissions, and k_r is the reaction term for CO_2.

The following boundary conditions were applied to reflect realistic atmospheric dispersion of CO_2 and were formally presented in recent studies of atmospheric dispersion and boundary effects (Jia *el al.,* 2025).

Boundary conditions:

i. **Source condition:** The pollutant is emitted continuously at a constant rate Q from a point source located at $(x,y,z) = (0,0,H_e)$. At $x = 0$, emission rate $= Q[g/s]$. This source condition is incorporated via a Dirac delta function $\delta(y)\delta(z-H_e)$ in the governing equation to model a point source at height H. This is expressed mathematically as:

$$uC|_{x=0} = Q\delta(y)\delta(z-H_e)$$

ii. **Ground boundary (reflecting ground at $z = 0$ for all x and y):** No flux through the ground, that is, a perfect reflection occurs (assuming the pollutant does not deposit or get absorbed). This is mathematically expressed as:

$$\left.\frac{\partial C}{\partial z}\right|_{z=0} = 0$$

At $z = 0$, the solution is constructed as the sum of two plumes, that is:

$$\mathrm{C(x,y,z)} = \mathrm{C_{real}(x,y,z)} + \mathrm{C_{image}(x,y,z)}$$

The spatial dispersion of CO_2 emissions is modelled from point sources in an energy system under steady atmospheric conditions as stated below:

Mathematical assumptions

To simplify the problem, the following assumptions were made:

i. No pollutant was present in the atmosphere before the source began emitting CO_2.
ii. The system maintains a steady state, that is $\frac{\partial C}{\partial t} = 0$.
iii. The wind speed is high enough that advection dominates diffusion in the x–direction which implies that $D_x \approx 0$.
iv. The speed of the wind U is constant in the x–direction.
v. The terrain is flat and has an infinite domain.

Analytical Solution Using Collocation Technique

Considering the above assumptions, equation (1) is reduced to a parabolic Partial Differential Equation (PDE) as thus:

$$U\frac{\partial C}{\partial x} = D_y\frac{\partial^2 C}{\partial y^2} + D_z\frac{\partial^2 C}{\partial z^2} + S(x,y,z) - k_r C \quad (2)$$

Applying the first boundary condition for a continuous point source at height H, $S(x,y,z) = Q\delta(y)\delta(z-H)$. Substituting into equation (2) gives:

$$U\frac{\partial C}{\partial x} = D_y\frac{\partial^2 C}{\partial y^2} + D_z\frac{\partial^2 C}{\partial z^2} + Q\delta(y)\delta(z-H) - k_r C \quad (3)$$

Because pollutant dispersion in the crosswind and vertical directions is well described by Gaussian distributions (Seinfeld and Pandis, 2016; Stockie, 2011), we assume an initial approximate trial solution as thus:

$$\mathrm{C(x,y,z)} \approx \mathrm{A(x)exp}[-\alpha(x)y^2 - \beta(x)(z-H)^2] \quad (4)$$

Let $F(x,y,z) = exp[-\alpha(x)y^2 - \beta(x)(z-H)^2]$. Therefore, equation (4) becomes:

$$\mathrm{C(x,y,z)} = \mathrm{A(x)}\,F(x,y,z) \quad (5)$$

The derivatives $\frac{\partial C}{\partial x}$, $\frac{\partial^2 C}{\partial y^2}$ and $\frac{\partial^2 C}{\partial z^2}$ of equation (5) are obtained as thus:

$$\frac{\partial C}{\partial x} = A'(x)F + A(x)\frac{\partial F}{\partial x}$$

Since $\frac{\partial F}{\partial x} = -F[\alpha'(x)y^2 + \beta'(x)(z-H)^2]$

$$\therefore \frac{\partial C}{\partial x} = A'(x)F - A(x)F[\alpha'(x)y^2 + \beta'(x)(z-H)^2] \quad (6a)$$

Also,

$$\frac{\partial C}{\partial y} = A(x)\frac{\partial F}{\partial y}$$

Since $\frac{\partial F}{\partial y} = -2\alpha(x)yF$

$$\therefore \frac{\partial C}{\partial y} = -2A(x)\alpha(x)yF$$

The second derivative $\frac{\partial^2 C}{\partial y^2}$ is obtained thus:

$$\frac{\partial^2 C}{\partial y^2} = -2A(x)\alpha(x)\left[F + y\frac{\partial F}{\partial y}\right]$$

$$\frac{\partial^2 C}{\partial y^2} = -2A(x)\alpha(x)[F + (-2\alpha(x)y^2F)]$$

$$\therefore \frac{\partial^2 C}{\partial y^2} = A(x)F[4\alpha^2(x)y^2 - 2\alpha(x)] \quad (6b)$$

Similarly,

$$\frac{\partial C}{\partial z} = A(x)\frac{\partial F}{\partial z}$$

Since $\frac{\partial F}{\partial z} = -2\beta(x)(z-H)F$

$$\therefore \frac{\partial C}{\partial z} = -2A(x)\beta(x)(z-H)F$$

The second derivative $\frac{\partial^2 C}{\partial z^2}$ is obtained thus:

$$\frac{\partial^2 C}{\partial z^2} = -2A(x)\beta(x)\left[F + (z-H)\frac{\partial F}{\partial z}\right]$$

$$\frac{\partial^2 C}{\partial z^2} = -2A(x)\beta(x)[F - (2\beta(x)(z-H)^2F)]$$

$$\frac{\partial^2 C}{\partial z^2} = A(x)F[4\beta^2(x)(z-H)^2 - 2\beta(x)] \quad (6c)$$

Substituting equations (6a), (6b) and (6c) into equation (2) gives:

$$U\left[A'(x)F - A(x)F[\alpha'(x)y^2 + \beta'(x)(z-H)^2]\right] = D_y[A(x)F(4\alpha^2(x)y^2 - 2\alpha(x))] + D_z[A(x)F(4\beta^2(x)(z-H)^2 - 2\beta(x))] + Q\delta(x)\delta(y)\delta(z-H) - k_r A(x)F \quad (7)$$

Equation (7) is reduced by dividing through by $A(x)F$

$$U\left[\frac{A'(x)}{A(x)} - [\alpha'(x)y^2 + \beta'(x)(z-H)^2]\right] = D_y[(4\alpha^2(x)y^2 - 2\alpha(x))] + D_z[(4\beta^2(x)(z-H)^2 - 2\beta(x))] + \frac{Q\delta(x)\delta(y)\delta(z-H)}{A(x)F} - k_r$$

(8)

The Gaussian factor is nonzero and equation (8) holds for all y and z. The coefficients of the independent polynomial factors 1, y^2 and $(z-H)^2$ in equation (8) ae compared. That is, $Q\delta(x)\delta(y)\delta(z-H)=0$. This reduces equation (8) to:

$$U\left[\frac{A'(x)}{A(x)}-[\alpha'(x)y^2+\beta'(x)(z-H)^2]\right]=D_y[(4\alpha^2(x)y^2-2\alpha(x))]+D_z[(4\beta^2(x)(z-H)^2-2\beta(x))]-k_r \quad (9)$$

Matching the coefficients of the constant terms in equation (9) gives:

$$U\frac{A'(x)}{A(x)}=-2D_y\alpha(x)-2D_z\beta(x)-k_r$$

$$\therefore \frac{A'(x)}{A(x)}=\frac{-2D_y\alpha(x)-2D_z\beta(x)-k_r}{U} \quad (10a)$$

Also, matching the coefficients of y^2gives:

$$-U\alpha'(x)=4D_y\alpha^2(x)$$

$$\therefore \alpha'(x)=-\frac{4D_y}{U}\alpha^2(x) \quad (10b)$$

Similarly, matching the coefficients of $(z-H)^2$ gives:

$$-U\beta'(x)=4D_z\beta^2(x)$$

$$\therefore \beta'(x)=-\frac{4D_z}{U}\beta^2(x) \quad (10c)$$

The Ordinary Differential Equations (ODEs) (10a), (10b) and (10c) come from collocation on the 3 test functions 1, y^2 and $(z-H)^2$. The collocation enforces the PDE in space spanned by those moments.

Change of variable is performed by defining:

$$\sigma_y^2=\frac{1}{2\alpha} \text{ and } \sigma_z^2=\frac{1}{2\beta}$$

Differentiating both sides of σ_y^2 and σ_z^2 with respect to x using chain rule gives:

$$\left.\begin{aligned}\frac{d}{dx}(\sigma_y^2)=\frac{d}{dx}\left(\frac{1}{2\alpha}\right)=-\frac{1}{2\alpha^2}\left(\frac{d\alpha}{dx}\right)\\ \frac{d}{dx}(\sigma_z^2)=\frac{d}{dx}\left(\frac{1}{2\beta}\right)=-\frac{1}{2\beta^2}\left(\frac{d\beta}{dx}\right)\end{aligned}\right\} \quad (11)$$

Substituting $\alpha'(x)$ and $\beta'(x)$ from equations (10b) and (10c) into equation (11) gives:

$$\left.\begin{aligned}\frac{d}{dx}(\sigma_y^2)=-\frac{1}{2\alpha^2}\left(-\frac{4D_y}{U}\alpha^2(x)\right)=\frac{2D_y}{U}\\ \frac{d}{dx}(\sigma_z^2)=-\frac{1}{2\beta^2}\left(-\frac{4D_z}{U}\beta^2(x)\right)=\frac{2D_z}{U}\end{aligned}\right\} \quad (12)$$

Integrating equation (12) with respect to x gives:

$$\left.\begin{aligned}\sigma_y^2=\int_0^x\frac{2D_y}{U}dx=\frac{2D_y}{U}x+B_1\\ \sigma_z^2=\int_0^x\frac{2D_z}{U}dx=\frac{2D_z}{U}x+B_2\end{aligned}\right\} \quad (13)$$

Where B_1 and B_2 are the integration constants.

Implementing the initial condition at $x=0$, $\sigma_y^2(0)=\sigma_z^2(0)=0$. Therefore $B_1=B_2=0$. This implies that:

$$\left.\begin{aligned}\sigma_y^2=\frac{2D_y}{U}x\\ \sigma_z^2=\frac{2D_z}{U}x\end{aligned}\right\} \quad (14)$$

Recall that $\sigma_y^2 = \frac{1}{2\alpha}$ and $\sigma_z^2 = \frac{1}{2\beta}$. Therefore, making α and β the subject of formula in the above, we have:

$$\left.\begin{array}{l} \alpha = \frac{1}{2\sigma_y^2} \\ \\ \beta = \frac{1}{2\sigma_z^2} \end{array}\right\} \quad (15)$$

Solving for the amplitude equation $\frac{A'(x)}{A(x)} = \frac{-2D_y\alpha(x) - 2D_z\beta(x) - k_r}{U}$, we substitute for α and β as thus:

$$\frac{A'(x)}{A(x)} = \frac{-2D_y\left(\frac{1}{2\sigma_y^2}\right) - 2D_z\left(\frac{1}{2\sigma_z^2}\right) - k_r}{U} \quad (16)$$

Reducing equation (16) gives:

$$\frac{A'(x)}{A(x)} = \frac{-\frac{D_y}{\sigma_y^2} - \frac{D_z}{\sigma_z^2} - k_r}{U} \quad (17)$$

Substituting equation (14) into equation (17),

$$\frac{A'(x)}{A(x)} = \frac{-\frac{D_y}{\frac{2D_y}{U}x} - \frac{D_z}{\frac{2D_z}{U}x} - k_r}{U} \quad (18)$$

Simplifying equation (18) gives:

$$\frac{A'(x)}{A(x)} = \frac{-\frac{U}{2x} - \frac{U}{2x} - k_r}{U} \quad (19)$$

Simplifying further,

$$\frac{A'(x)}{A(x)} = -\frac{1}{x} - \frac{k_r}{U} \quad (20)$$

Integrating both sides of equation (20) with respect to x,

$$\int \frac{A'(x)}{A(x)} dx = \int \left(-\frac{1}{x} - \frac{k_r}{U}\right) dx \quad (21)$$

Note that $A'(x) = \frac{dA}{dx}$, substituting into equation (21),

$$\int \frac{1}{A(x)} dA = \int \left(-\frac{1}{x} - \frac{k_r}{U}\right) dx \quad (22)$$

$$\ln A = -\ln x - \frac{k_r}{U}x + C_0 \quad (23)$$

Taking the exponential of both sides gives:

$$e^{\ln A} = e^{-\ln x} \cdot e^{-\frac{k_r}{U}x} \cdot e^{C_0} \quad (24)$$

$$\Rightarrow A = \frac{B}{x} e^{-\frac{k_r}{U}x} \quad (25)$$

Where $B = e^{C_0}$

To get the concentration value C, the cross-plane mass (the total mass of pollutant per unit length along the x-axis at any specific distance) is defined as:

$$M(x) = \iint_{-\infty}^{\infty} C(x, y, z) dydz \quad (26)$$

The concentration $C(x, y, z)$ satisfies an advection-diffusion reaction equation. Integrating equation (26) over y and z, the diffusion terms vanishes due to decay at infinity as thus:

$$\iint_{-\infty}^{\infty} \left[U \frac{\partial C}{\partial x}\right] dydz = \iint_{-\infty}^{\infty} \left[D_y \frac{\partial^2 C}{\partial y^2} + D_z \frac{\partial^2 C}{\partial z^2} + S(x, y, z) - k_r C\right] dydz \quad (27)$$

Recall that for $x > 0$, $S(x, y, z) = Q\delta(x)\delta(y)\delta(z - H) = 0$. This reduces equation (27) to:

$$\iint_{-\infty}^{\infty} \left[U \frac{\partial C}{\partial x}\right] dydz = \iint_{-\infty}^{\infty} \left[D_y \frac{\partial^2 C}{\partial y^2} + D_z \frac{\partial^2 C}{\partial z^2} - k_r C\right] dydz \quad (28)$$

$$U \frac{d}{dx} \iint_{-\infty}^{\infty} C \, dydz = D_y \iint_{-\infty}^{\infty} \frac{\partial^2 C}{\partial y^2} dydz + D_z \iint_{-\infty}^{\infty} \frac{\partial^2 C}{\partial z^2} dydz - k_r \iint_{-\infty}^{\infty} C \, dydz \quad (29)$$

Recall that $M(x) = \iint_{-\infty}^{\infty} C(x, y, z) dydz$. Therefore:

$$U\frac{dM}{dx} = D_y \iint_{-\infty}^{\infty} \frac{\partial^2 C}{\partial y^2} dydz + D_z \iint_{-\infty}^{\infty} \frac{\partial^2 C}{\partial z^2} dydz - k_r M \quad (30)$$

Analyzing the diffusion terms $\iint_{-\infty}^{\infty} \frac{\partial^2 C}{\partial y^2} dydz$ and $\iint_{-\infty}^{\infty} \frac{\partial^2 C}{\partial z^2} dydz$ and integrating one variable at a time as thus:

$$\iint_{-\infty}^{\infty} \frac{\partial^2 C}{\partial y^2} dydz = \int \left[\int_{-\infty}^{\infty} \frac{\partial^2 C}{\partial y^2} dy\right] dz = \int \left[\frac{\partial C}{\partial y}\right]_{-\infty}^{\infty} dz \quad (31a)$$

Similarly,

$$\iint_{-\infty}^{\infty} \frac{\partial^2 C}{\partial z^2} dydz = \int \left[\int_{-\infty}^{\infty} \frac{\partial^2 C}{\partial z^2} dz\right] dy = \int \left[\frac{\partial C}{\partial z}\right]_{-\infty}^{\infty} dy \quad (31b)$$

A fundamental requirement of the Gaussian plume model is that the concentration C and its derivatives go to zero at infinity. That is $\left[\frac{\partial C}{\partial y}\right]_{-\infty}^{\infty} = \left[\frac{\partial C}{\partial z}\right]_{-\infty}^{\infty} = 0$. Equations (31a) and (31b) therefore become zero. Substituting into equation (30),

$$U\frac{dM}{dx} = -k_r M \quad (32)$$

Equation (32) is a first order ODE in $M(x)$. Solving the ODE,

$$\frac{dM}{dx} = -\frac{k_r}{U} M \quad (33)$$

Employing separation of variables,

$$\frac{dM}{M} = -\frac{k_r}{U} dx$$

Integrating both sides,

$$\ln M = -\frac{k_r}{U} x + C_1$$

Taking exponential of both sides:

$$M = e^{-\frac{k_r}{U}x} \cdot e^{C_1}$$

Since mass is a positive value, we let $M_0 = e^{C_1}$, which represent the mass per unit length just downstream of the source. Therefore:

$$M(x) = M_0 e^{-\frac{k_r}{U}x} \quad (34)$$

The source emits mass at a rate Q. The mass flow rate in the x-direction is $UM(x)$, so at $x = 0$, $UM_0 = Q$

$$\therefore M_0 = \frac{Q}{U} \quad (35)$$

Substituting equation (35) into equation (34),

$$M(x) = \frac{Q}{U} e^{-\frac{k_r}{U}x} \quad (36)$$

We compute $M(x)$ from the Gaussian form of $C(x,y,z)$ as thus:

$$\iint_{-\infty}^{\infty} C(x,y,z) dydz = M(x) = \iint_{-\infty}^{\infty} \left[\mathrm{A(x)} \exp[-\alpha(x)y^2 - \beta(x)(z-H)^2]\right] dydz \quad (37)$$

Integrating the right-hand side with respect to $dydz$,

$$M(x) = \mathrm{A(x)} \int_{-\infty}^{\infty} e^{-\alpha y^2} dy \int_{-\infty}^{\infty} e^{-\beta(z-H)^2} dz \quad (38)$$

Using the standard Gaussian integral

$$\int_{-\infty}^{\infty} e^{-au^2} du = \sqrt{\frac{\pi}{a}}$$

Therefore,

$$M(x) = \mathrm{A(x)} \cdot \sqrt{\frac{\pi}{\alpha}} \cdot \sqrt{\frac{\pi}{\beta}}$$

(39)

$$\therefore M(x) = \mathrm{A(x)} \frac{\pi}{\sqrt{\alpha\beta}} \quad (40)$$

Recall from equation (15) that $\alpha = \frac{1}{2\sigma_y^2}$ and $\beta = \frac{1}{2\sigma_z^2}$, substituting into equation (40) gives;

$$M(x) = \mathrm{A(x)} \frac{\pi}{\sqrt{\frac{1}{2\sigma_y^2} \cdot \frac{1}{2\sigma_z^2}}} \quad (41)$$

Simplifying equation (41),

$$M(x) = 2\pi\sigma_y\sigma_z \mathrm{A(x)} \quad (42)$$

Equating equation (42) to equation (36) gives;

$$2\pi\sigma_y\sigma_z \mathrm{A(x)} = \frac{Q}{U} e^{-\frac{k_r}{U}x} \quad (43)$$

Making $A(x)$ the subject of formula,

$$\mathrm{A(x)} = \frac{Q}{2\pi\sigma_y\sigma_z U} e^{-\frac{k_r}{U}x} \quad (44)$$

Substituting equation (44) back into our assumed trial solution (equation (4)) gives;

$$\mathrm{C(x,y,z)} \approx \frac{Q}{2\pi\sigma_y\sigma_z U} e^{-\frac{k_r}{U}x} \exp[-\alpha(x)y^2 - \beta(x)(z-H)^2] \quad (45)$$

Substituting the values of $\alpha = \frac{1}{2\sigma_y^2}$ and $\beta = \frac{1}{2\sigma_z^2}$ into equation (45) gives;

$$\mathrm{C(x,y,z)} \approx \frac{Q}{2\pi\sigma_y\sigma_z U} e^{-\frac{k_r}{U}x} \exp\left[-\frac{y^2}{2\sigma_y^2} - \frac{(z-H)^2}{2\sigma_z^2}\right] \quad (46)$$

Implementing the ground boundary condition gives;

$$\mathrm{C(x,y,z)} \approx \frac{Q}{2\pi\sigma_y\sigma_z U} e^{-\frac{k_r}{U}x} \exp\left[-\frac{y^2}{2\sigma_y^2}\right] \cdot \left[exp\left(-\frac{(z-H)^2}{2\sigma_z^2}\right) + exp\left(-\frac{(z+H)^2}{2\sigma_z^2}\right)\right] \quad (47)$$

The equation (47) above is the approximate collocation solution for the concentration of CO_2 in the atmosphere at any spatial location incorporating a first-order reaction term. This solution is exactly the same as the analytical solution and therefore confirms the reliability of the analytical solution and also establishes confidence in the use of the model for practical application.

Results and Discussion

The Figures 1 – 5 below were obtained by implementing equation (47) on MAPLE 2023.0 software. The following baseline parameters were used: $Q = 30.61\mathrm{kg/s}$, $U = 3\,m/s$, $H_e = 50\,m$, $k_r = 0.00001\,1/m$ and the dispersion coefficients $\sigma_y(x)$ and $\sigma_z(x)$ used are for stability class-D as captured on the Pasquill-Gifford table (Turner, 1994). For each sensitivity analysis, a single parameter was perturbed over a specified range, whereas all other parameters were fixed at their baseline values to isolate its individual effect on the plume concentration field.

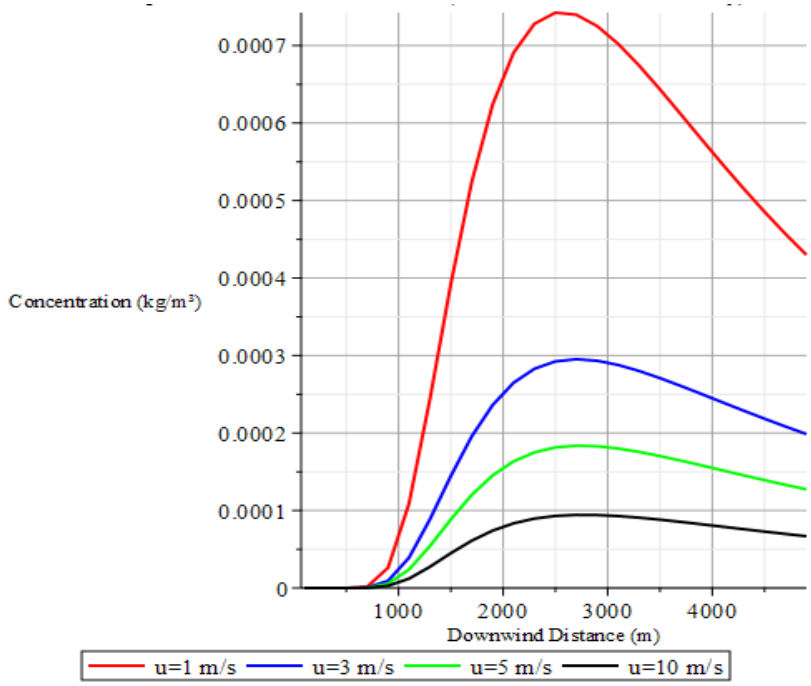

Figure 1: Plot Showing the Influence of Wind Speed on CO_2 Downwind Concentration

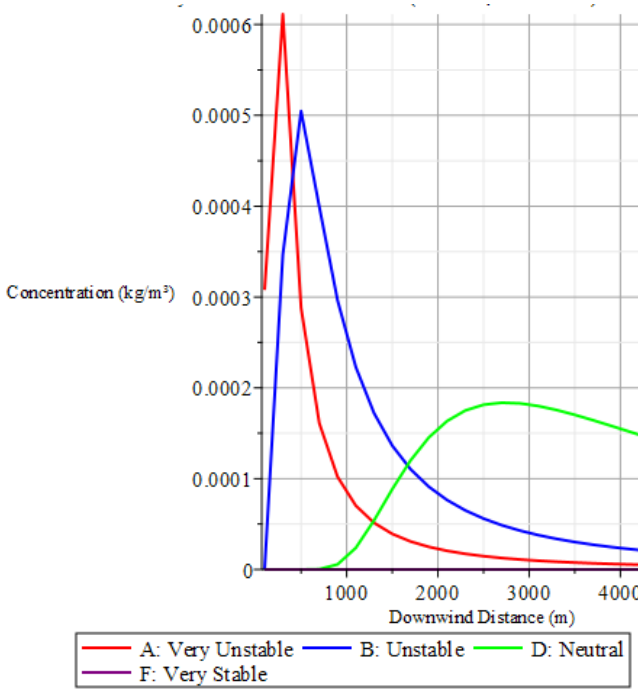

Figure 2: Plot Showing the Influence of Stability Class on CO_2 Concentration Downwind.

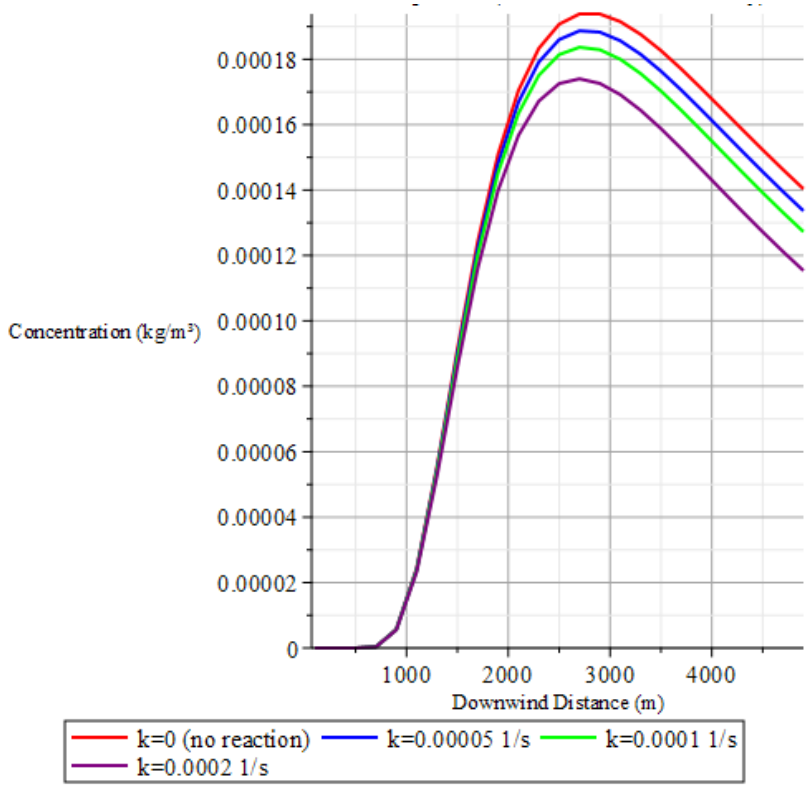

Figure 3: Plot Showing the Influence of Reaction Term on CO_2 Concentration Downwind.

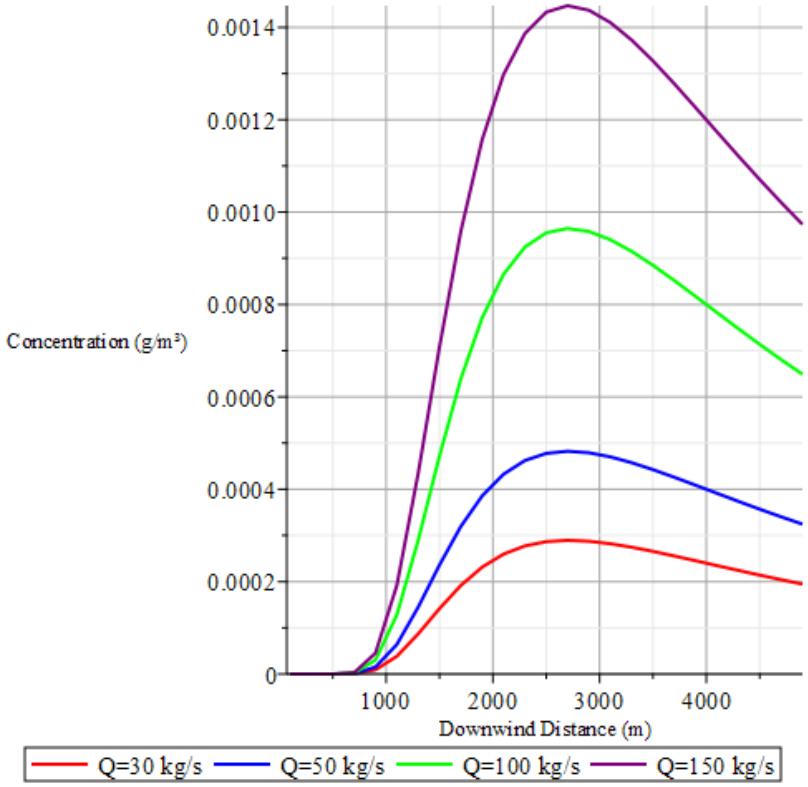

Figure 4: Plot Showing the Influence of Emission Rate on CO_2 Concentration Downwind.

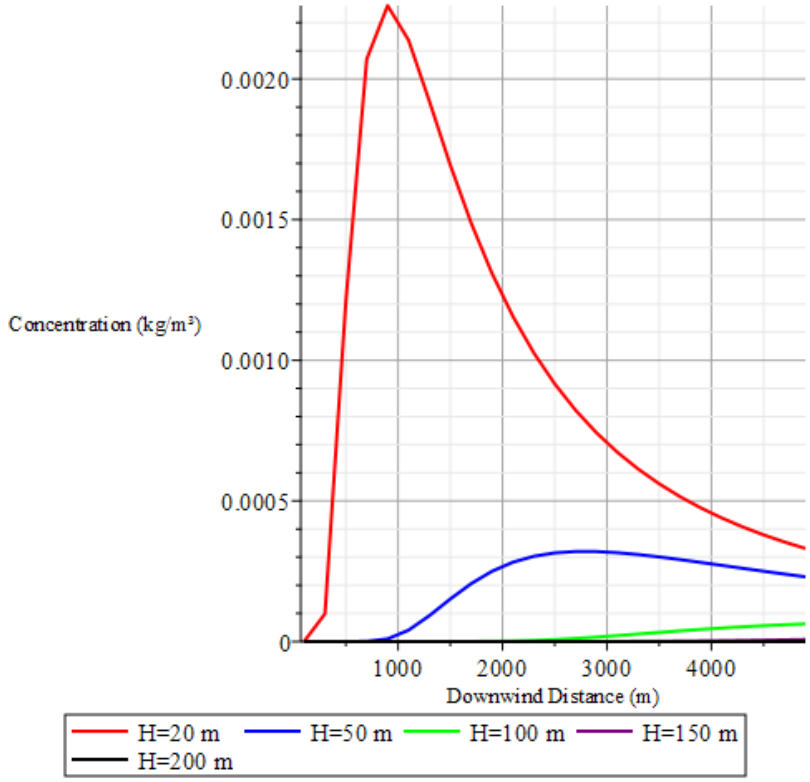

Figure 5: Plot Showing the Influence of Stack Height on CO_2 Concentration Downwind.

The results presented above provides insight into how source characteristics and meteorological conditions influence dispersion behaviour and identifies conditions under which elevated concentrations are most likely to occur.

Figure 1 shows that increasing wind speed leads to a marked reduction in ground-level CO_2 concentration. This behaviour is consistent with the advective scaling of the Gaussian plume model, in which higher wind speeds transport the plume more rapidly downstream and enhance dilution by spreading the pollutant over a larger volume of air. Consequently, lower wind speeds result in higher near-field concentrations and represent less favourable dispersion conditions. This highlights the importance of meteorological variability in environmental impact assessments, particularly in regions where calm or low-wind conditions are frequent.

A as illustrated in Figure 2, atmospheric stability strongly influences vertical and horizontal mixing. Under unstable conditions, enhanced turbulent mixing increases the vertical and lateral spread of the plume, leading to lower peak concentrations near the ground but a wider spatial footprint. Conversely, stable atmospheric conditions suppress turbulence, limit vertical mixing, and promote higher concentrations near the ground within a narrower plume. The observed differences between stability classes underscore the importance of incorporating atmospheric stability into dispersion modelling, especially when assessing worst-case exposure scenarios.

The inclusion of a first-order reaction term introduces exponential reduction of concentration with distance, as shown in Figure 3. Although CO_2 is often treated as chemically inert on short timescales, the reaction term can be interpreted more generally as representing effective removal processes, such as biological uptake, chemical transformation, or numerical damping. The observed reduction in concentration with increasing reaction rate confirms the expected mathematical behaviour of the model.

Figure 4 indicates a direct proportionality between emission rate and concentration magnitude, while the spatial location of the maximum impact zone remains largely unchanged. This reflects the linearity of the governing equation with respect to the source term and implies that changes in emission rate primarily scale concentration levels without altering the plume geometry. This finding suggests that emission control strategies are effective for reducing absolute concentration levels but do not necessarily change the spatial extent of exposure.

Figure 5 illustrates the influence of stack height, showing that higher release points substantially reduce ground-level concentrations by allowing greater vertical dispersion before the plume reaches the surface. This confirms a fundamental principle of air pollution control: increasing effective stack height promotes atmospheric dilution and reduces near-field exposure. However, while taller stacks reduce local impacts, they may increase the geographical range of pollutant transport, which should be considered in regional-scale assessments.
Collectively, the results identify a zone of elevated ground-level CO_2 concentration approximately between 2000m and 5000m downwind of the source under typical operating conditions. This region represents a critical exposure zone that is sensitive to both meteorological conditions and operational parameters. The identification of this zone has practical implications for land-use planning, environmental monitoring, and regulatory decision-making.

Conclusion

This study developed and applied a localized Gaussian plume model to assess the dispersion of atmospheric CO_2 emitted from the Ibom Power Thermal Plant under steady-state conditions. An analytical solution of the governing advection–diffusion–reaction equation was derived using a collocation-based approximation framework, thereby validating the mathematical formulation and demonstrating the consistency of the numerical approach. Sensitivity analysis revealed that wind speed, atmospheric stability, emission rate, reaction rate, and stack height significantly influence both the magnitude and spatial distribution of ground-level CO_2 concentrations. A key outcome of the analysis is the identification of a critical impact zone located approximately between 2000m to 5000m downwind of the plant, where ground-level CO_2 concentrations are predicted to be highest under typical conditions. This zone represents a region of heightened exposure risk and provides a quantitative basis for guiding land-use planning, environmental monitoring, and the siting of sensitive receptors such as residential areas, schools, and healthcare facilities.

Future work may extend the approach to include stochasticity, time-dependent meteorology, complex terrain, and interactions with other atmospheric processes. Nonetheless, the results demonstrate that Gaussian-based dispersion modelling remains a valuable and computationally efficient tool for environmental impact assessment of thermal power plants.

References

Abiye, O. E., Sunmonu, L. A., Ajao, A. I., Akinola, O. E., Ayoola, M. A., & Jegede, O. O. (2016). Atmospheric dispersion modeling of uncontrolled gaseous pollutants (SO_2 and NO_X) emission from a scrap-iron recycling factory in Ile-Ife, Southwest Nigeria. *Cogent Environmental Science,* 2(1). https://doi.org/10.1080/23311843.2016.1275413

Al-Naser, R., & Khalaf, M. (2025). Assessment of air pollution resulting from the South Baghdad power plant using the Gaussian model. *Journal of Agrometeorology*, 27. https://doi.org/10.54386/jam.v27i1.2759

Alvarez, R. A., Zavala-Araiza, D., Lyon, D. R., Allen, D. T., Barkley, Z. R., Brandt, A. R. & Hamburg, S. P. (2018). Assessment of methane emissions from the U.S. oil and gas supply chain. *Science*, 361(6398), 186–188. https://doi.org/10.1126/science.aar7204

Awodumi, O. B., & Adewuyi, A. O. (2020). The role of non-renewable energy consumption in economic growth and carbon emission: Evidence from oil producing economies in Africa. *Energy Strategy Reviews,* 27, 100434, ISSN 2211-467X. https://doi.org/10.1016/j.esr.2019.100434

Emodi, N. V., & Boo, K. J. (2017). Energy policy for sustainable development in Nigeria: A review of the energy landscape, policy framework and indicators. *Renewable and Sustainable Energy Reviews*, 69, 291–301. https://doi.org/10.1016/j.rser.2016.11.117

Happiness, R. O., Ogunniran, B. I., & Oluleye, A. (2019). Modeling of gaseous pollutants dispersion of a fossil fuel-fired power plant at Omotosho, Ondo State, Nigeria. *Advancement in Science and Technology Research*, 5(2), 9–36. https://www.researchgate.net/publication/379685647

I.E.A. (2023). CO_2 emissions in 2022. Retrieved from https://www.iea.org/reports/co2-emissions-in-2022.0

Jia, M., Fish, R., Daniels, W. S., Sprinkle, B., & Hammerling, D. (2025). A fast and lightweight implementation of the Gaussian puff model for near-field atmospheric transport of trace gasses. *Scientific Reports,* 15(1), 18710. https://doi.org/10.1038/s41598-025-99491-x

Lacome, J. M., Leroy, G., Joubert, L., & Truchot, B. (2023). Harmonisation in atmospheric dispersion modelling approaches to assess toxic consequences in the neighbourhood of industrial facilities. *Atmosphere,* 14(11), 1605. https://doi.org/10.3390/atmos14111605

Lupini, R., & Tirabassi, T. (1967). Gaussian plume model and advection-diffusion equation: An attempt to connect the two approaches. *Atmospheric Environment,* Volume 13(8), Pages 1169-1174. https://doi.org/10.1016/0004-6981(79)90041-6

Nunes, L. J. R. (2023). The rising threat of the atmospheric CO2: a review on the causes, impacts, and mitigation strategies. *Environments,* 10(4), 66. https://doi.org/10.3390/environments10040066

Pantusheva, M., Mitkov, R., Hristov, P. O., & Petrova-Antonova, D. (2022). Air pollution dispersion modelling in urban environment using CFD: A systematic review. *Atmosphere,* 13(10), 1640. https://doi.org/10.3390/atmos13101640

Seinfeld, J. H., & Pandis, S. N. (2016). *Atmospheric Chemistry and Physics: From Air Pollution to Climate Change* (3rd Edition). Wiley, New Jersey. ISBN 978-1-118-94740-1. https://www.wiley.com/en-us/Atmospheric+Chemistry+and+Physics

The Guardian. (2015). NERC issues licence to Ibom Power for 685 MW plant. *The Guardian Nigeria*. Retrieved from https://guardian.ng/energy/nerc-issues-licence-to-ibom-power-for-685mw-plant/

Turner, D. B. (1994). *Workbook of atmospheric dispersion estimates: An introduction to dispersion modeling.* (2nd edition). CRC Press, Cincinnati.

United States Environmental Protection Agency (USEPA). (2025). Greenhouse gas emissions from a typical passenger vehicle. Retrieved from https://www.epa.gov/greenvehicles